The High Temperature Phases of Multiferroic $BiFe_{0.7}Mn_{0.3}O_3$

Alexandra S. Gibbs,[1,2] Donna C. Arnold,[1,3] Kevin S. Knight,[4] and Philip Lightfoot[1,*]

[1] *School of Chemistry and EaStCHEM, University of St Andrews, North Haugh, St Andrews KY16 9ST, United Kingdom*

[2] *Scottish Universities Physics Alliance (SUPA), School of Physics and Astronomy, University of St Andrews, North Haugh, St Andrews KY16 9SS, United Kingdom*

[3] *School of Physical Sciences, University of Kent, Canterbury, Kent, CT2 7NH, United Kingdom*

[4] *ISIS Facility, Rutherford Appleton Laboratory, Chilton, Didcot OX11 OQX, United Kingdom*

We report the results of a high-resolution powder neutron diffraction study of multiferroic $BiFe_{0.7}Mn_{0.3}O_3$. We have confirmed the previous assignment of the α-phase and β-phase as having $R3c$ and $Pbnm$ symmetry, respectively. The γ-phase, however, has been shown unequivocally not to be cubic, as previously reported, but rather to retain octahedral tilting distortions leading to a lower symmetry, most likely rhombohedral with space group $R\bar{3}c$. The γ-phase of $BiFe_{0.7}Mn_{0.3}O_3$ is therefore different to that of the parent $BiFeO_3$ which retains an orthorhombic structure up to its decomposition temperature. The lattice parameters of the γ-phase of $BiFe_{0.7}Mn_{0.3}O_3$ are pseudo-cubic throughout its entire stability range despite the fact that there are still significant distortions from the cubic aristotype structure even at the onset of decomposition.

PACS numbers: 61.05.fm,61.50.Ks,75.85.+t

I. INTRODUCTION

$BiFeO_3$ is one of the most well-studied of the multiferroic materials, partly due to the fact that it is in the multiferroic state at room temperature with coexisting antiferromagnetic and ferroelectric orders. Despite this, the details of its high-temperature phase transitions have only recently been resolved[1,2] and the details of its low-temperature structural and magnetic properties are still debated. The pure compound has three structural phases at and above room temperature. The ferroelectric α-phase, which is multiferroic below T_N=643 K, has the space group $R3c$ (although recent work has suggested a very subtle monoclinic[3] or even triclinic[4] distortion) and is stable from low temperature up to $T_{\alpha-\beta}$=1093 K. The orthorhombic β-phase with space group $Pbnm$ (non-standard setting of $Pnma$) is stable up to $T_{\beta-\gamma}$ =1198 K[1] and the γ-phase exists in the small window between $T_{\beta-\gamma}$ and the decomposition temperature of 1223 K[2].

Many dopants have been used to modify or stabilise the properties of $BiFeO_3$ and also to try to gain insight into the underlying physics of the undoped parent compound[5–7]. Substitution of Mn^{3+} for Fe^{3+} increases the magnetization and dielectric constant although T_N and T_C are lower than in the pure compound[5,8,9]. The Mn-substituted compound $BiFe_{0.7}Mn_{0.3}O_3$ has been reported, based upon x-ray diffraction, differential thermal analysis (DTA), dilatometry and conductivity data, to have lower transition temperatures than the parent compound: $T_{\alpha-\beta}$=943 K and $T_{\beta-\gamma}$ =1160 K, with peritectic decomposition reported at 1193 K[10,11]. The Néel temperature is also decreased to T_N=533 K. $BiFe_{0.7}Mn_{0.3}O_3$, when prepared at ambient pressure, is reported to adopt the same α and β phases as the parent $BiFeO_3$; however, the γ-phase has been reported to be cubic, unlike the parent compound, with the aristotype $Pm\bar{3}m$ structure[10,11]. Under high pressure synthesis conditions a different, $PbZrO_3$-like, orthorhombic form is stabilised at ambient temperature[12,13]. The γ-phase of $BiFeO_3$ has been reported to be metallic[14] whereas the β- and γ-phases of $BiFe_{0.7}Mn_{0.3}O_3$ are semiconducting[11]. Both the α-to-β and β-to-γ transition were confirmed to be first order in nature by DTA[10,11].

Since the only diffraction studies of the high-temperature phases so far have used x-ray powder diffraction a neutron diffraction experiment was carried out to determine whether the increased sensitivity of the technique to oxygen atom positions could shed any further light on the high temperature phases of $BiFe_{0.7}Mn_{0.3}O_3$.

II. EXPERIMENTAL

A. Sample Synthesis and Characterisation

Samples of $BiFe_{0.7}Mn_{0.3}O_3$ were synthesised by the rapid liquid phase sintering technique. This method has been used previously for both pure $BiFeO_3$ and $BiFe_{0.7}Mn_{0.3}O_3$ as the liquid Bi_2O_3 at the sintering temperature ensures quick reaction which reduces loss of volatile Bi_2O_3 and impurity phases due to the metastability of $BiFeO_3$ and $BiFe_{0.7}Mn_{0.3}O_3$ towards mullite and sillenite-type compounds $Bi_2Fe_{4-x}Mn_xO_9$ and $Bi_{25}Fe_{1-y}Mn_yO_{39}$ at the sintering temperature. The appropriate ratios of the reactant oxide powders Bi_2O_3, Fe_2O_3 and Mn_2O_3 were mixed and acetone-ground to ensure small particle size and through mixing. The powder was then compressed into small pellets and sintered in a pre-heated furnace at 1173 K for 10 minutes followed by quenching in air to room temperature. Previous reports by Selbach *et al.* have found that this preparation method (quenching in air from 1173 K) results in samples of $BiFe_{0.7}Mn_{0.3}O_{3+\delta}$ with $\delta = 0.030 \pm 0.005$[10,11]. No separate analysis of the oxygen nonstoichiometry was

performed by us. During the Rietveld refinements of the neutron powder diffraction data refinement of the cation site occupancies gave a variation of less than 1.5% and no detectable improvement in the fit.

B. Powder Neutron Diffraction

Powder neutron diffraction experiments were carried out on the high-resolution instrument HRPD at ISIS. The samples were sealed in an evacuated quartz tube, placed in a vanadium can, which was then mounted in a standard RAL furnace. Data were taken at 44 temperatures between room temperature and 1191 K. Appropriate equilibration times were included upon each temperature change. In the β-phase short data collection times, corresponding to 15 μAh incident proton beam, were used for most runs to ensure that in the metastable region transformation to the mullite and sillenite phases was minimised. These were interspersed with longer runs of 50 μAh at 913 K, 963 K, 1013 K, 1113 K and 1153 K. In the γ-phase 30 μAh exposures were recorded per dataset up to 1173 K and 8 μAh at each temperature above except for at 1173 K where 50 μAh was collected and 1191 K where 10 μAh was collected.

The data used for analysis were taken from the back-scattering bank and additionally from the 90°-bank for analysis of the β-phase. Data were refined using the Rietveld method as implemented in GSAS[15].

III. RESULTS

The room-temperature diffraction patterns confirmed the phase purity of the sample, with no additional peaks observed beyond those belonging to vanadium from the sample can. The previous assignment by Selbach *et al.*[10,11] and Sosnowska *et al.*[16] of space group $R3c$ for the α-phase was also confirmed, with no evidence of symmetry lowering as recently suggested for $BiFeO_3$. A substantial amount of anisotropic broadening was present, however, with a variation of more than a factor of two between the full-width half-maxima of some peaks (see supplemental material[17] for further details). A Rietveld refinement for the 523 K dataset, including terms for anisotropic broadening, gave a satisfactory fit as can be seen in figure 1. The results of the refinement are tabulated in table I and a Crystallographic Information File (CIF) is included in the supplemental material[17] . Due to the instrumental characteristics of HRPD, which is optimised for low d-spacing structural studies, and the time-of-flight window used for the experiment (30-130 ms), detailed study of the magnetic structure was not possible. One pure magnetic reflection was observed below T_N at 4.58 Å which could correspond to the (101/003) reflection observed by Sosnowska *et al.* for $BiFe_{0.8}Mn_{0.2}O_3$[18].

Atom	Site	x	y	z	U_{iso} ×100(Å^2)	Occ.
Bi	6a	0	0	0	1.94(7)	1
Fe	6a	0	0	0.22620(17)	1.63(10)	0.7
Mn	6a	0	0	0.22620(17)	1.63(10)	0.3
O1	18b	0.4504(4)	0.0180(4)	0.95600(19)	2.27(7)	1

TABLE I. The Rietveld refinement results of the $R3c$ model (including anisotropic broadening) for the α-phase of $BiFe_{0.7}Mn_{0.3}O_3$ at 523 K. The lattice parameters are a = 5.58833(16) Å and c = 13.8588(5) Å. The Bi z-parameter was kept fixed during the refinement to define the origin of the polar axis. The refinement gave R_{wp}=0.0307, χ^2=2.143 for 41 variables. Further details of the refined variables can be found in the supplemental material [17].

A. The α-to-β Transition

The transition from the α-phase to β-phase is clear upon visual examination of the diffraction patterns. As can be seen in figure 2, the (2,0,-4) peak of the rhombohedral phase is not visible above 963 K.

The previous assignment of $Pnma$ as the space group of the β-phase is confirmed by our data. In-depth investigation of other possible space groups based upon analysis of superlattice reflections of the perovskite aristotype structure[19,20] failed to find any model with a significantly better fit. This analysis relates distortions around different high symmetry points in the Brillouin zone to fractional-index reflections of the $Pm\bar{3}m$ cubic aristotype structure. The distortions are labelled with the irreducible representation of the distortion mode.

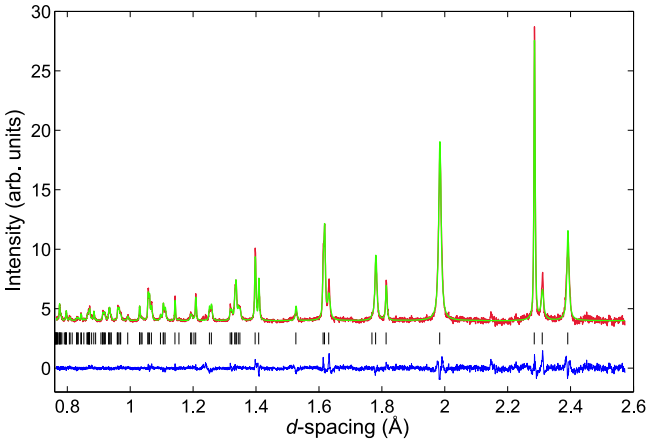

FIG. 1. (Colour Online) The Rietveld refinement for the 523 K dataset with space group $R3c$ including anisotropic broadening. The observed datapoints are plotted in red, the calculated profile in green and the difference profile in blue. The black ticks mark the expected reflection positions for the $R3c$ space group. The small additional peaks, for example at 2.15 Å, are from the vanadium sample can.

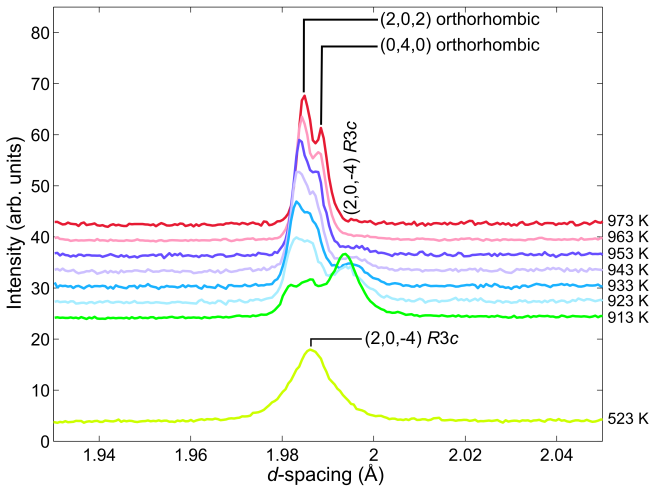

FIG. 2. (Colour Online) The diffraction patterns taken across the α-to-β transition of $BiFe_{0.7}Mn_{0.3}O_3$. There is coexistence of the rhombohedral and orthorhombic phases between 913 K and 953 K. The transition is complete by 963 K as evidenced by the disappearance of the (2,0,-4) peak.

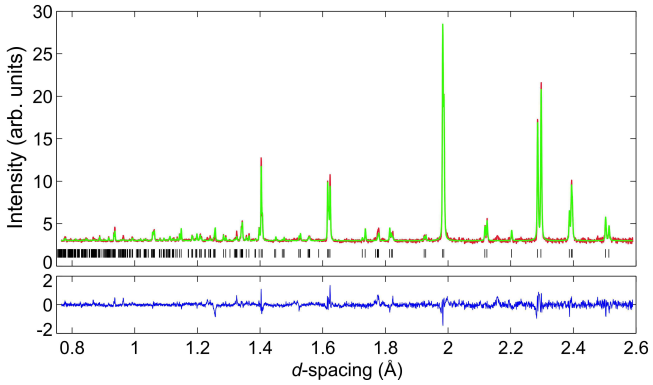

FIG. 3. (Colour Online) The Rietveld refinement results for the 963 K data in the β-phase of $BiFe_{0.7}Mn_{0.3}O_3$ in space group *Pnma*. The observed datapoints are plotted in red, the calculated profile in green and the difference profile in blue. The black ticks mark the expected reflection positions for the *Pnma* space group.

Atom	Site	x	y	z	U_{iso} $\times 100(Å^2)$	Occ.
Bi	4c	0.9773(4)	0.25	0.5033(4)	8.34(9)	1
Fe	4a	0	0	0	4.16(9)	0.7
Mn	4a	0	0	0	4.16(9)	0.3
O1	4c	0.0165(5)	0.25	0.0660(4)	6.06(11)	1
O2	8d	0.2902(3)	0.9634(2)	0.2088(3)	7.68(11)	1

TABLE II. The Rietveld refinement results of the *Pnma* model for the β-phase at 963 K. The lattice parameters are a = 5.62738(14) Å, b = 7.94594(18) Å and c = 5.58786(14) Å. The refinement gave R_{wp}(bank 1)=0.0276, R_{wp}(bank 2)=0.0264, χ^2=4.447 for 69 variables.

The relevant distortion modes of the $Pm\bar{3}m$ structure are R_4^+, M_3^+, X_5^+ and Γ_4^-. The superlattice reflections index as $(h,k,l)_{parent} \pm \left(\frac{1}{2},\frac{1}{2},\frac{1}{2}\right)$ for R_4^+-mode distortions, $(h,k,l)_{parent} \pm \left(\frac{1}{2},0,\frac{1}{2}\right)$ for M_3^+-point distortions and $(h,k,l)_{parent} \pm \left(0,\frac{1}{2},0\right)$ for X_5^+-mode distortions. Γ_4^--mode distortions do not produce superlattice peaks but instead modify the intensities of the aristotype peaks. Structurally the R_4^+-mode peaks correspond to out-of-phase tilts of adjacent octahedra and the M_3^+-mode peaks to analogous in-phase tilts. The X_5^+-mode peaks appear as a consequence of the presence of both R_4^+ and M_3^+ mode distortions. Γ_4^--mode distortions are composed of polar cation displacements. The possible space groups for perovskites with combinations of these distortion modes have been tabulated (for simple distortions) by Howard, Stokes *et al.*[21,22]. Four space groups are possible for concurrent R_4^+ and M_3^+-mode distortions and a further twelve for R_4^+, M_3^+ and Γ_4^--mode distortions[22]. Of these 16 space groups 8 were ruled out by the diffraction pattern violating either lattice symmetry or centring conditions. Of the remaining 8 a further four were ruled out by a lack of peak splitting necessitating such low symmetry. The remaining space groups were *Pnma* and its polar subgroups $Pmn2_1$, $Pmc2_1$ and $Pna2_1$.

The *Pnma* model (corresponding to Glazer notation $a^-b^+a^-$) gave a good fit with R_{wp}=0.0276, χ^2=4.447 for 69 variables. The results of the Rietveld refinement are shown in figure 3 and in table II and a Crystallographic Information File (CIF) is included in the supplemental material[17] . The polar subgroups of *Pnma* gave satisfactory fits, as can be seen in the supplemental material[17] . Indeed, both $Pmc2_1$ and $Pmn2_1$ gave somewhat lower R_{wp} and χ^2 values than *Pnma*. However, under visual inspection the difference in the fits was very small (see supplemental material[17]). Comparisons of each of these models over the entire temperature range of the β-phase failed to show any significant improvement on lowering the symmetry. In the absence of a significant improvement over *Pnma*, and of any physical property measurements indicating the necessity of a polar space group, *Pnma* was judged to be the most appropriate space group for the β-phase of $BiFe_{0.7}Mn_{0.3}O_3$.

We have therefore confirmed that, in agreement with previous reports[10,23], the α- and β-phases of $BiFe_{0.7}Mn_{0.3}O_3$ are isostructural to those of pure $BiFeO_3$, adopting space groups $R3c$ and *Pnma* respectively.

B. The β-to-γ Transition

Due to the isostructural nature of $BiFe_{0.7}Mn_{0.3}O_3$ and $BiFeO_3$ in the α-phase and β-phases it might be expected that the γ-phases would also be isostructural. Selbach *et al.*, however, have previously reported the γ-phase of $BiFe_{0.7}Mn_{0.3}O_3$ to adopt the perovskite aristotype cubic

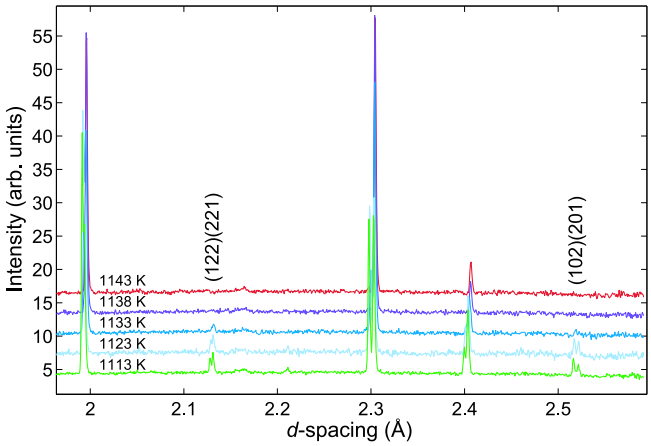

FIG. 4. (Colour Online) A range of the diffraction data across the β-to-γ transition of $BiFe_{0.7}Mn_{0.3}O_3$. The peaks labelled, which disappear in the γ-phase, correspond to M_3^+-mode distortions. The small, broad peak just above d =2.15 Å is from the vanadium sample can.

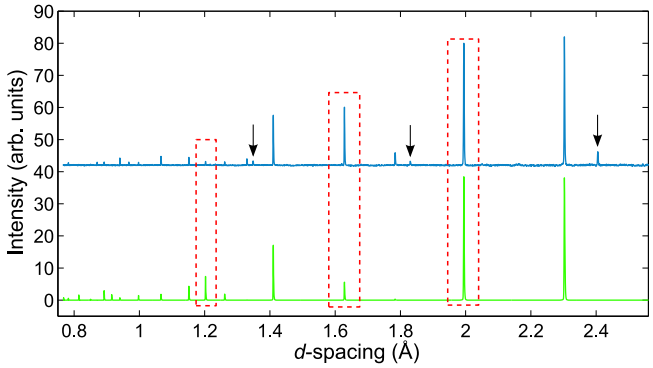

FIG. 5. (Colour Online) The predicted pattern for the cubic aristotype $Pm\bar{3}m$ structure (lower, green) and the diffraction pattern for T = 1153 K in the γ-phase (upper, blue). The arrows mark the peaks due to R_4^+ mode distortions. The red dotted boxes indicate peaks for which the the observed intensities differ strongly relative to those predicted for the cubic aristotype structure.

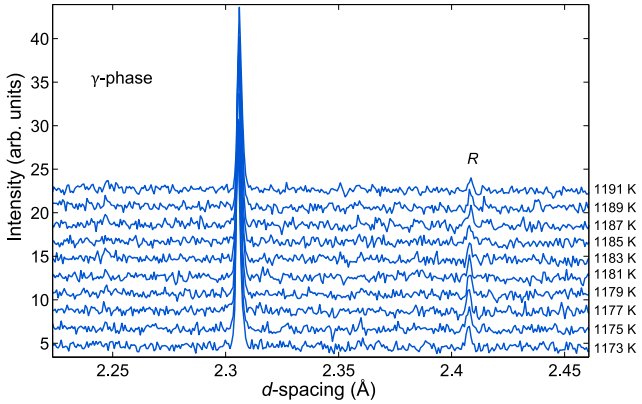

FIG. 6. (Colour Online) The highest-temperature data taken in the γ-phase of $BiFe_{0.7}Mn_{0.3}O_3$. The label 'R' indicates one of the R_4^+-mode peaks still present at the highest temperature measured. As the sample was beginning to decompose at the highest temperature with no indication of a phase transition being seen it seems that the aristotype cubic phase is not reached within the stability range of $BiFe_{0.7}Mn_{0.3}O_3$.

structure (space group $Pm\bar{3}m$) based upon x-ray powder diffraction data[11].

The transition to the γ-phase is clear in our diffraction data as can be seen in figure 4. There is a disappearance of M_3^+ and X_5^+ mode peaks which also correspond to body-centred systematic absences for the same orthorhombic unit cell, at and above 1138 K. This is in clear contrast to the parent compound $BiFeO_3$ which retains an orthorhombic structure up to its decomposition point.

Additionally, it is also clear that the γ-phase of $BiFe_{0.7}Mn_{0.3}O_3$ is *not* cubic. This is shown by the continued presence of R_4^+ mode distortion peaks as shown in figure 5. The presence of these peaks gives, from the analysis of Stokes *et al.*[22] (based upon simple tilt systems), the possible space groups $I4/mcm$, $Imma$, $R\bar{3}c$, $C2/m$, $C2/c$ and $P\bar{1}$ corresponding to Glazer tilt systems $a^0a^0c^-$, $a^0b^-b^-$, $a^-a^-a^-$, $a^0b^-c^-$, $a^-a^-c^-$, $a^-b^-c^-$). Although the symmetry is clearly lower than cubic, the lattice parameters are metrically cubic within experimental error for all datasets in the γ-phase.

It can also be seen in figure 5 that the intensities of the aristotype reflections differ substantially from those expected (unlike the β-phase). This could be due to either strongly anisotropic atomic displacement parameters or activity of polar Γ_4^- mode distortions.

Inspection of the highest temperature data, shown in figure 6 gives no sign of a further phase transition with R-point distortion peaks visible up to the highest temperatures measured where signs of decomposition became evident.

To identify the space group of the γ-phase, refinements of all of the candidate space group models were undertaken. Monoclinic and triclinic space groups were ruled out due to a lack of any splitting of the extremely narrow peaks which would necessitate such a low-symmetry structure. The remaining three space groups, $I4/mcm$, $Imma$ and $R\bar{3}c$, correspond to the presence of equal adjacent out-of-phase tilts along one, two or three axes respectively.

The tetragonal space group $I4/mcm$ could be ruled out by the unphysical U_{iso} values produced by the refinement. The inclusion of anisotropic thermal displacement parameters did not improve the fit and again resulted in physically unreasonable values.

The best fits with physically reasonable parameters were given by the $Imma$ and $R\bar{3}c$ models. Both of these space groups gave good fits with no peaks unindexed. The atomic displacement parameters were rather large for both space groups but not unreasonable as can be seen in table III. The atomic displacement parame-

Space Group	R_{wp}	χ^2	Oxygen Site $100 \times U_{iso}$ (Å^2)
$I4/mcm$	0.0319	3.365 (36 var.)	O1: 37.7(17)
			O2: 5.84(18)
$Imma$	0.0327	3.535 (36 var.)	O1: 6.9(3)
			O2: 11.5(3)
$R\bar{3}c$	0.0362	4.331 (33 var.)	O1: 7.88(12)

TABLE III. The R_{wp}, χ^2 and oxygen atom U_{iso} values for the fully isotropic $R\bar{3}c$, $I4/mcm$ and $Imma$ refinements for the γ-phase at 1153 K.

Atom	Wyckoff Position	x	y	z	$100 \times U_{iso}$ (Å^2)	Occ.
Bi	6a	0	0	0.25	7.81(11)	1
Fe	6b	0	0	0.5	1.23(6)	0.7
Mn	6b	0	0	0.5	1.23(6)	0.3
O	18e	0.4585(5)	0	0.25	7.88(12)	1

TABLE IV. The Rietveld refinement results of the $R\bar{3}c$ isotropic model for the γ-phase at 1153 K. The lattice parameters are $a = 5.63969(19)$ Å, $c = 13.8146(8)$ Å. The refinement gave R_{wp}=0.0362, χ^2=4.331 for 33 variables. The results for the anisotropic model can be seen in the supplemental information.

ter for the single oxygen site in the $R\bar{3}c$ refinement is smaller than for the equatorial O2 site in the $Imma$ model. Due to this, and also the fact that $R\bar{3}c$ is a higher symmetry structure than $Imma$ we conclude that space group $R\bar{3}c$ provides the best model for the γ-phase of $BiFe_{0.7}Mn_{0.3}O_3$. This choice is supported further by carrying out comparative anisotropic refinements for these two space groups. The most significant improvements were found by allowing the O atoms to refine anisotropically leading to R_{wp} and χ^2 values of R_{wp}=0.0218, χ^2=1.572 for 42 variables and R_{wp}=0.0222, χ^2=1.634 for 38 variables for the $Imma$ and $R\bar{3}c$ models respectively.

The choice of $R\bar{3}c$ over $Imma$ is also indirectly supported by the first order nature of the β-to-γ transition as seen in the discontinuity in the unit cell volume. To allow ease of visualisation of the unit cell volume throughout the temperature-dependent phase diagram these were normalised to those of the pseudo-cubic unit cell, corresponding to the perovskite aristotype cell (thus allowing comparison of volumes for unit cells with equal numbers of formula units). The resulting trend in V_c is shown in figure 7. This trend across the phase diagram is in general agreement with that reported by Selbach *et al.*[10,11] with a decrease in volume across the α-to-β transition and an increase across the β-to-γ transition. The abrupt volume changes are consistent with the first order nature of both transitions. With respect to the β-to-γ transition, this clear evidence of the first order nature points towards the correct space group for the γ-phase being $R\bar{3}c$ rather than

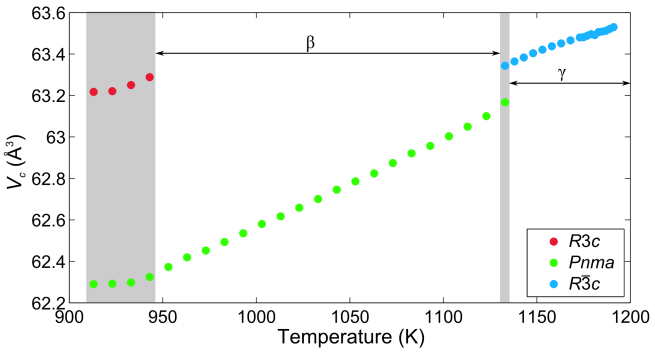

FIG. 7. (Colour Online) The normalised unit cell volumes for the high-temperature phases of $BiFe_{0.7}Mn_{0.3}O_3$. The volumes plotted are normalised per formula unit for all phases. The areas shaded grey indicate phase coexistence.

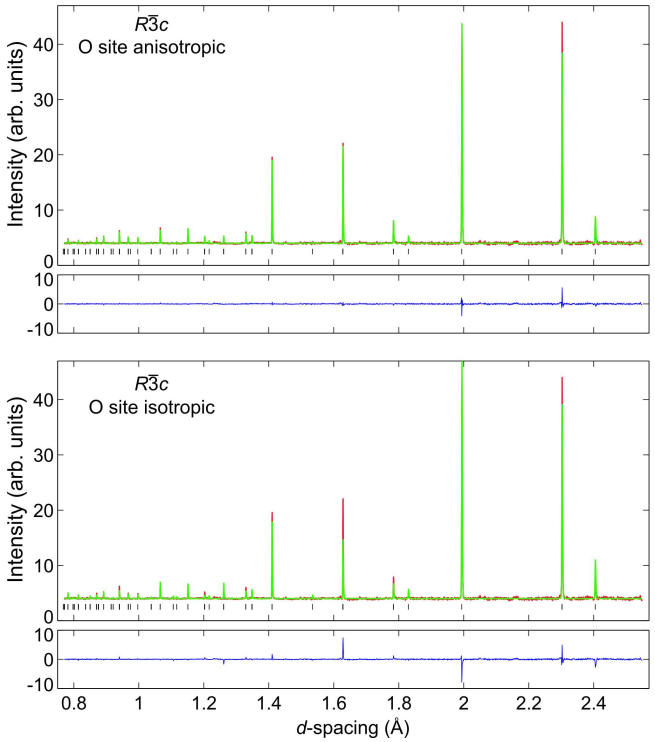

FIG. 8. (Colour Online) The results of the Rietveld refinements of the $R\bar{3}c$ model for the γ-phase of $BiFe_{0.7}Mn_{0.3}O_3$ at 1153 K. The observed datapoints are plotted in red, the calculated profile in green and the difference profile in blue. The black ticks mark the expected reflection positions for the $R3c$ space group. The upper panel shows the results of the refinement with anisotropic atomic displacement parameters for the oxygen site and the lower panel the result from all sites treated isotropically.

$Imma$ as the transition $Pnma$-$R\bar{3}c$ must be first order by Landau theory[21] and is accompanied by a clear volume discontinuity in systems such as $LaGaO_3$[24,25]. The transition $Pnma$-$Imma$, however, is allowed to be second order by Landau theory and in other perovskite systems such as $SrRuO_3$ this transition shows no clear disconti-

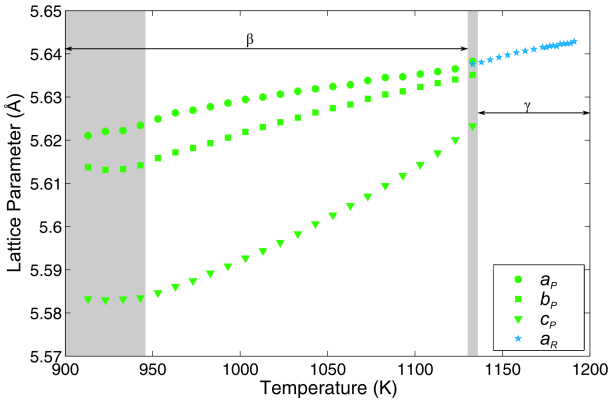

FIG. 9. (Colour Online) The lattice parameters for the β- and γ-phases of $BiFe_{0.7}Mn_{0.3}O_3$. The lattice parameters from the β-phase (a_P, b_p and c_p) are those of the $Pnma$ unit cell and for the γ-phase the rhombohedral parameter, a_R, is used. This refers to the lattice parameters extracted from refinements in $R\bar{3}c$, since the lattice parameters are metrically cubic over the whole γ-phase $a_R = \sqrt{2}(c_R/(2\sqrt{3}))$. The areas shaded grey indicate phase coexistence.

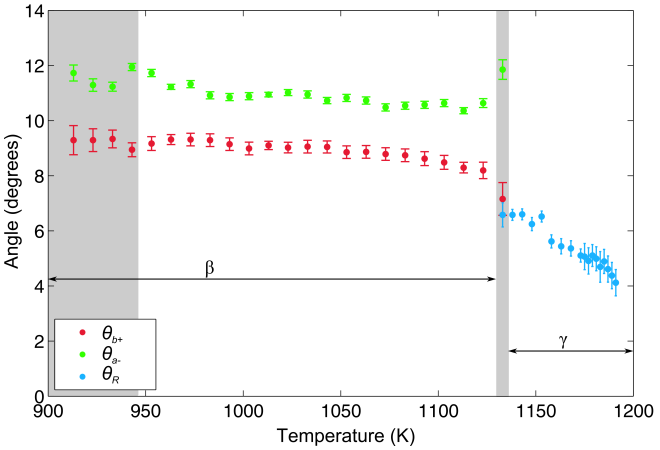

FIG. 10. (Colour Online) The octahedral tilt angles, as calculated by the method of Kennedy *et al.*[27], for the β- and γ-phases of $BiFe_{0.7}Mn_{0.3}O_3$. The tilt angle would only be expected to go to zero for temperatures above $T = 1200$ K. The areas shaded grey indicate phase coexistence.

nuity in volume[26]. Although not conclusive, the clear discontinuity in volume across the β-to-γ transition indicates, in agreement with the crystallographic evidence, that $R\bar{3}c$ is the most likely space group for the γ-phase of $BiFe_{0.7}Mn_{0.3}O_3$.

Comparative results of two Rietveld refinements of the $R\bar{3}c$ model, respectively with fully isotropic atomic displacement parameters and with the oxygen site only refined anisotropically are shown in figure 8. The results of the fully isotropic refinement are tabulated in table IV. The results of the anisotropic refinement and a Crystallographic Information File (CIF) for the isotropically refined structure are included in the supplemental material[17] . Investigation of anisotropic refinement of the Bi site gave no significant deviation from an isotropic ellipsoid and no clear improvement to the quality of the fits.

Figure 9 shows the lattice parameters of the β and γ-phases, with the $R\bar{3}c$ model being used for the γ-phase. The lattice parameters increase smoothly throughout the β- and γ-phases. Interestingly, as previously mentioned, the lattice parameters are metrically cubic throughout the γ-phase.

Figure 10 shows the temperature dependence of the octahedral tilt angles through the β- and γ-phases. The tilt angle decrease with increasing temperature is consistent with the unit cell expansion seen in figure 9, but this will also have a contribution from bond expansion effects. The abrupt decrease in the average tilt angle at the beta-gamma transition apparently leads to the increase in unit cell volume observed at this point (figure 7); this behaviour contrasts with the unit cell volume decrease seen in $BiFeO_3$ itself at this point, previously ascribed to an insulator-metal transition[2].

The trend of the tilt angle at highest temperatures furthermore indicates that the tilt angle would not be expected to go to zero until above T=1200 K. This therefore confirms that a cubic phase of $BiFe_{0.7}Mn_{0.3}O_3$ is not realised within its stability range.

IV. CONCLUSIONS

In conclusion, we have confirmed the previous assignments of the α- and β-phases of $BiFe_{0.7}Mn_{0.3}O_3$ as rhombohedral (space group $R3c$) and orthorhombic (space group $Pnma$) respectively. However, we have shown conclusively that the previous assignment of cubic, $Pm\bar{3}m$, for the γ-phase was incorrect. Our neutron diffraction data provide a much more robust method of studying the behaviour of the key oxygen atom displacements, as compared to the previous x-ray studies. In particular, the present data highlight clearly the persistence of the R_4^+ octahedral tilt mode throughout the γ-phase, confirming that this phase cannot be cubic. Nevertheless, the γ-phase displays *metrically* cubic symmetry throughout its stability regime, making competing models in space groups $I4/mcm$, $Imma$ and $R\bar{3}c$ difficult to distinguish. $R\bar{3}c$ is suggested as the simplest and most physically reasonable model. The observation of clear octahedral tilts distortions in a metrically cubic perovskite is unusual but not unprecedented[28,29] and this merits further study by techniques more sensitive to local structural effects.

ACKNOWLEDGMENTS

The authors thank the EPSRC and STFC for funding.

* To whom correspondence should be addressed: pl@st-andrews.ac.uk

[1] D. C. Arnold, K. S. Knight, F. D. Morrison, and P. Lightfoot, Phys. Rev. Lett. **102**, 027602 (2009).

[2] D. C. Arnold, K. S. Knight, G. Catalan, S. A. T. Redfern, J. F. Scott, P. Lightfoot, and F. D. Morrison, Adv. Funct. Mater. **20**, 2116 (2010).

[3] I. Sosnowska, R. Przeniosło, A. Palewicz, D. Wardecki, and A. Fitch, J. Phys. Soc. Jpn. **81**, 044604 (2012).

[4] H. Wang, C. Yang, J. Lu, M. Wu, J. Su, K. Li, J. Zhang, G. Li, T. Jin, T. Kamiyama, F. Liao, J. Lin, and Y. Wu, Inorg. Chem. **52**, 2388 (2013).

[5] J. R. Sahu and C. N. R. Rao, Solid State Sci. **9**, 950 (2007).

[6] I. H. Ismailzade, R. M. Ismailov, A. I. Alekberov, and F. M. Salaev, Phys. Status Solidi A **68**, K81 (1981).

[7] X. Qi, J. Dho, R. Tomov, M. G. Blamire, and J. L. MacManus-Driscoll, Appl. Phys. Lett. **86**, 062903 (2005).

[8] C.-H. Yang, T. Y. Koo, and Y. H. Jeong, Solid State Commun. **134**, 299 (2005).

[9] D. Kothari, V. R. Reddy, A. Gupta, D. M. Phase, N. Lakshmi, S. K. Deshpande, and A. M. Awasthi, J. Phys.: Condens. Matter **19**, 136202 (2007).

[10] S. M. Selbach, T. Tybell, M.-A. Einarsrud, and T. Grande, Chem. Mater. **21**, 5176 (2009).

[11] S. M. Selbach, T. Tybell, M.-A. Einarsrud, and T. Grande, Phys. Rev. B **79**, 214113 (2009).

[12] M. Azuma, H. Kanda, A. A. Belik, Y. Shimakawa, and M. Takano, J. Magn. Magn. Mater. **310**, 1177 (2007).

[13] A. A. Belik, A. M. Abakumov, A. A. Tsirlin, J. Hadermann, J. Kim, G. Van Tendeloo, and E. Takayama-Muromachi, Chem. Mater. **23**, 4505 (2011).

[14] S. A. T. Redfern, J. N. Walsh, S. M. Clark, G. Catalan, and J. F. Scott, (2009), arXiv:0901.3748.

[15] A. C. Larson and R. B. Von Dreele, *General Structure Analysis System (GSAS)*, Tech. Rep. LAUR 86-748 (Los Alamos National Laboratory, 2000).

[16] I. Sosnowska, W. Schäfer, and I. O. Troyanchuk, Phys. B **276-278**, 576 (2000).

[17] See Supplemental Material at [URL will be inserted by publisher].

[18] I. Sosnowska, W. Schäfer, W. Kockelmann, K. H. Andersen, and I. O. Troyanchuk, Appl. Phys. A: Mater. Sci. Process. **74**, S1040 (2002).

[19] A. M. Glazer, Acta Crystallogr. Sec. A **31**, 756 (1975).

[20] C. J. Howard, R. L. Withers, K. S. Knight, and Z. Zhang, J. Phys.: Condens. Matter **20**, 135202 (2008).

[21] C. J. Howard and H. T. Stokes, Acta Crystallogr. Sec. B **54**, 782 (1998).

[22] H. T. Stokes, E. H. Kisi, D. M. Hatch, and C. J. Howard, Acta Crystallogr. Sec. B **58**, 934 (2002).

[23] S. M. Selbach, M.-A. Einarsrud, and T. Grande, Chem. Mater. **21**, 169 (2009).

[24] C. J. Howard and B. J. Kennedy, J. Phys.: Condens. Matter **11**, 3229 (1999).

[25] K. S. Knight, J. Solid State Chem. **194**, 286 (2012).

[26] B. Kennedy, B. Hunter, and J. Hester, Phys. Rev. B **65**, 224103 (2002).

[27] B. J. Kennedy, C. J. Howard, and B. C. Chakoumakos, J. Phys.: Condens. Matter **11**, 1479 (1999).

[28] B. J. Maier, R. J. Angel, W. G. Marshall, B. Mihailova, C. Paulmann, J. M. Engel, M. Gospodinov, A.-M. Welsch, D. Petrova, and U. Bismayer, Acta Crystallogr. Sec. B **66**, 280 (2010).

[29] B. J. Maier, R. J. Angel, B. Mihailova, W. G. Marshall, M. Gospodinov, and U. Bismayer, J. Phys.: Condens. Matter **23**, 035902 (2011).